Supplementary Information: Experimental observation and characterization of amorphous carbon generated for graphene on gold nanoparticles

Surjyasish Mitra[a], Natalie Hamada[b,] and Sushanta. K. Mitra[a,*]*

[a]*Department of Mechanical & Mechatronics Engineering, Waterloo Institute for Nanotechnology, University of Waterloo, Waterloo, Ontario N2L 3G1, Canada.*
[b] *Canadian Centre for Electron Microscopy, McMaster University, 1280 Main St W, Hamilton, ON L8S 4L8, Canada.*

*hamadan@mcmaster.ca
** skmitra@uwaterloo.ca

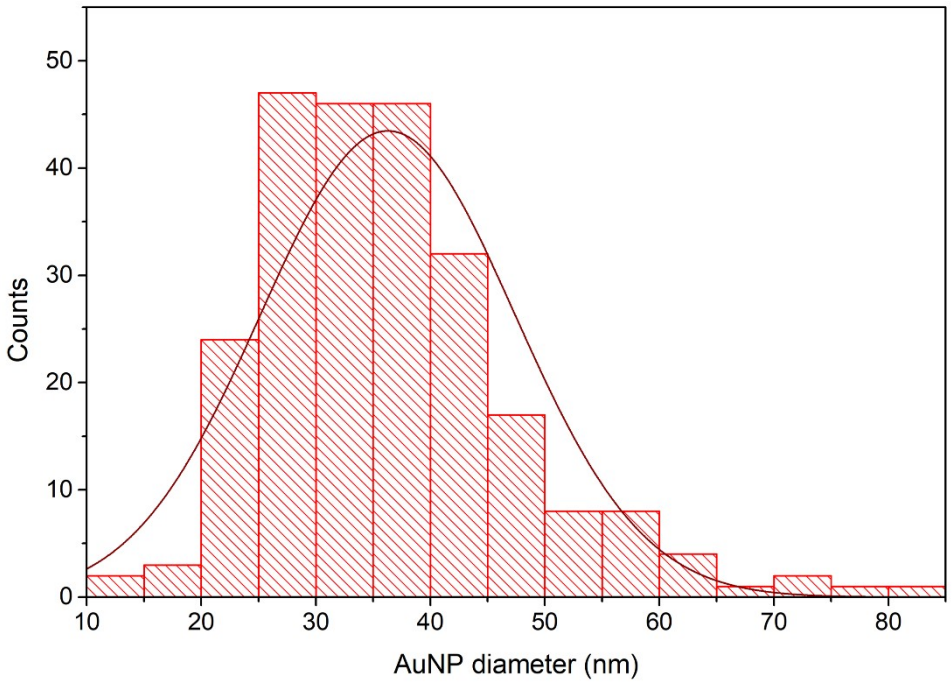

Figure S1: Particle size distribution of the gold nanoparticles (AuNPs) on the TEM grid analyzed using high magnification High-Resolution TEM (HRTEM) images. The solid curve represents the fitting of the normal distribution.

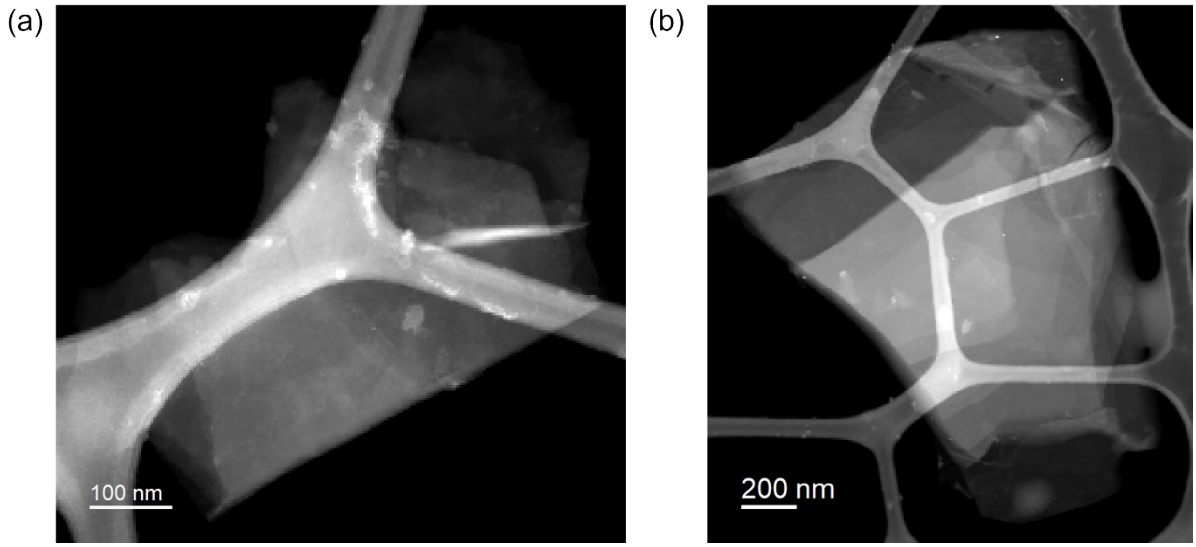

Figure S2: (a) and (b) High-Angle Annular Dark Field (HAADF) images of graphene-only samples, i.e., without gold nanoparticles.

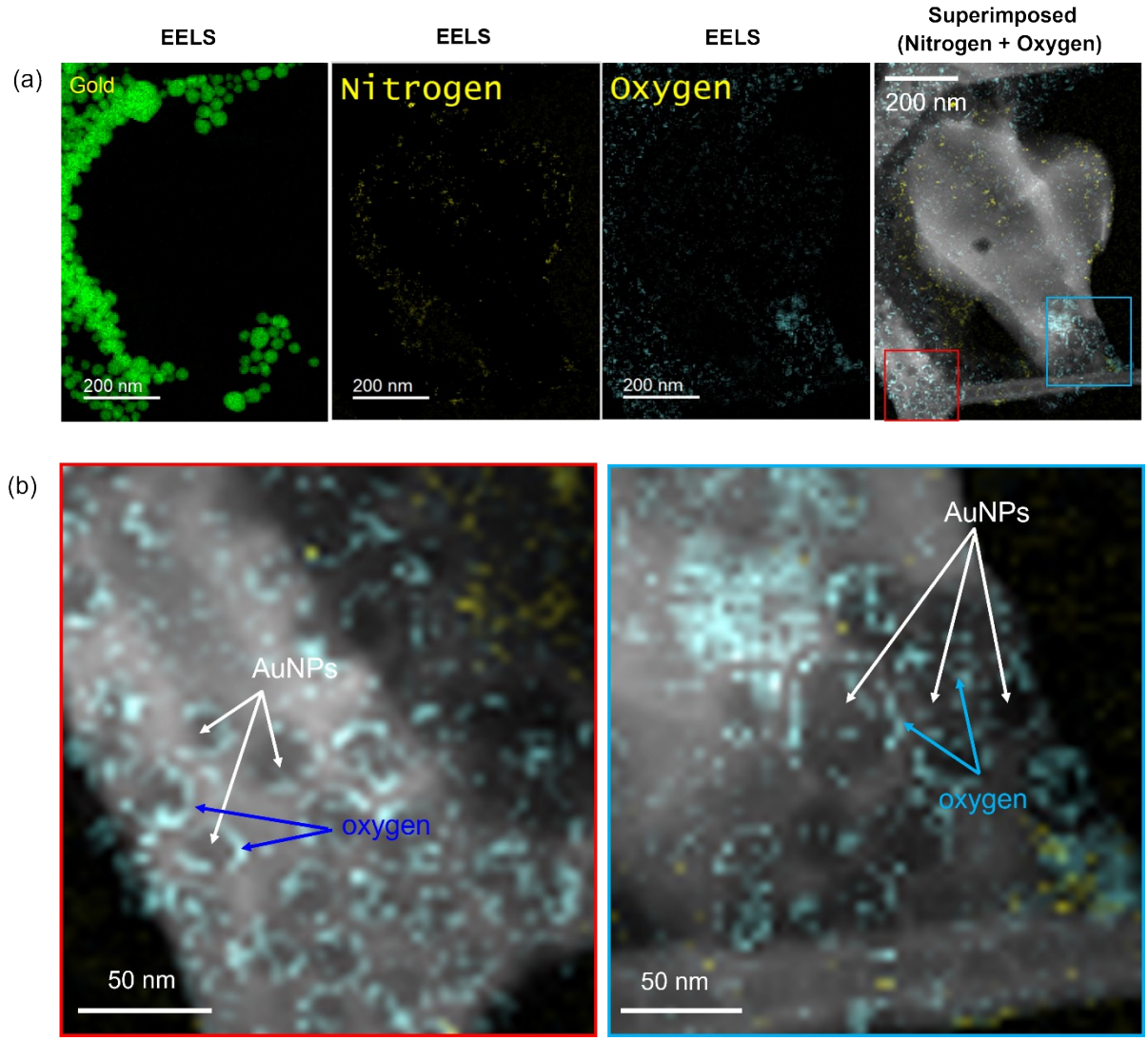

Figure S3: (a) Electron energy loss spectroscopy (EELS) signature of gold nanoparticles (AuNPs), adsorbed nitrogen, and oxygen corresponding to Figure 4 in the main text. Superimposed EELS signature of nitrogen and oxygen. (b) Enlarged views of the red and blue box regions in the superimposed signature. The oxygen appears to be on top of the AuNPs.

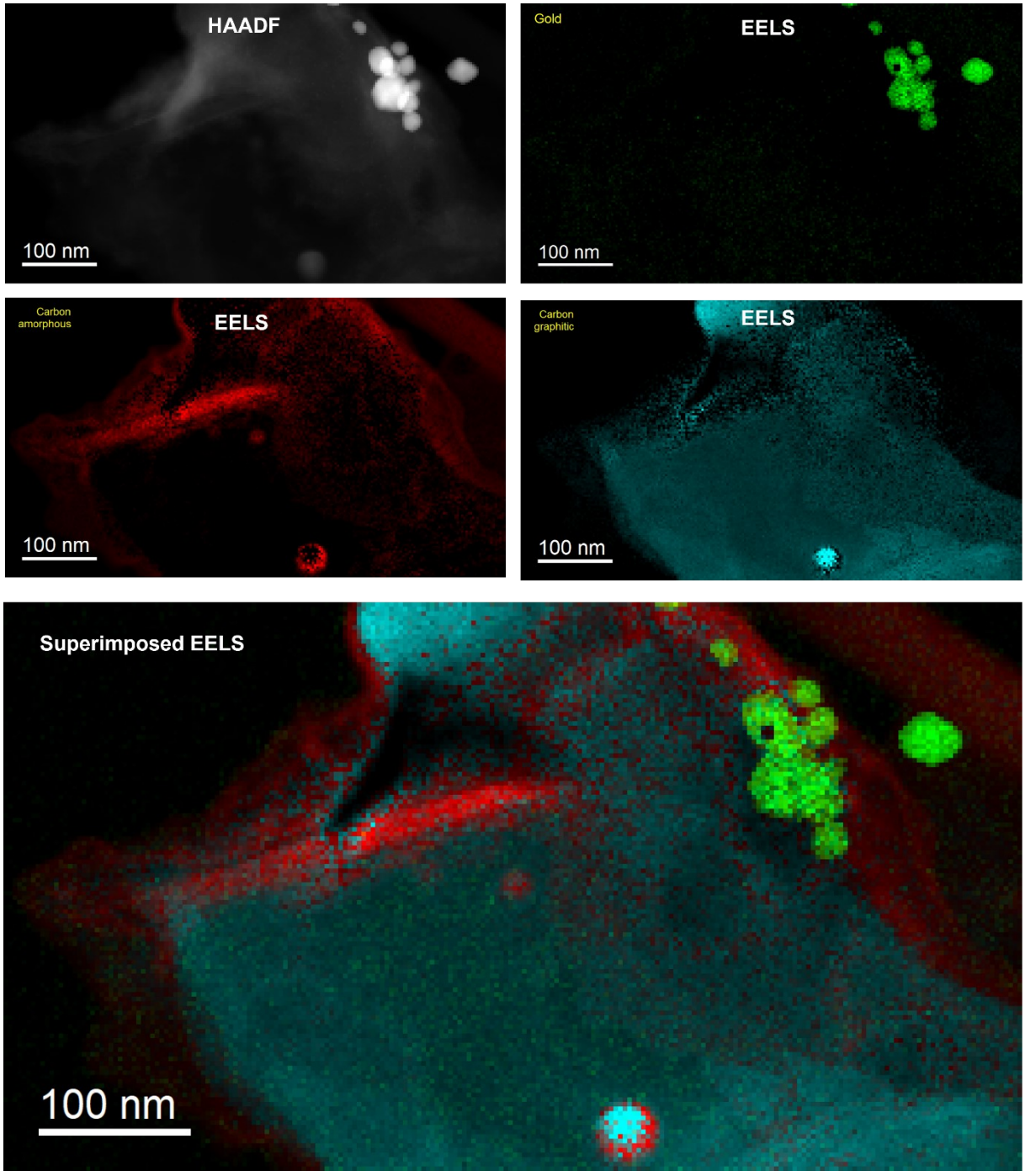

Figure S4: High-Angle Annular Dark Field (HAADF) image of graphene with gold nanoparticles (AuNPs) in the vicinity. Corresponding EELS elemental mapping signature of AuNPs, amorphous carbon, and graphitic carbon. The final image is the superimposed elemental map of all the elements. The color assignment is arbitrary.

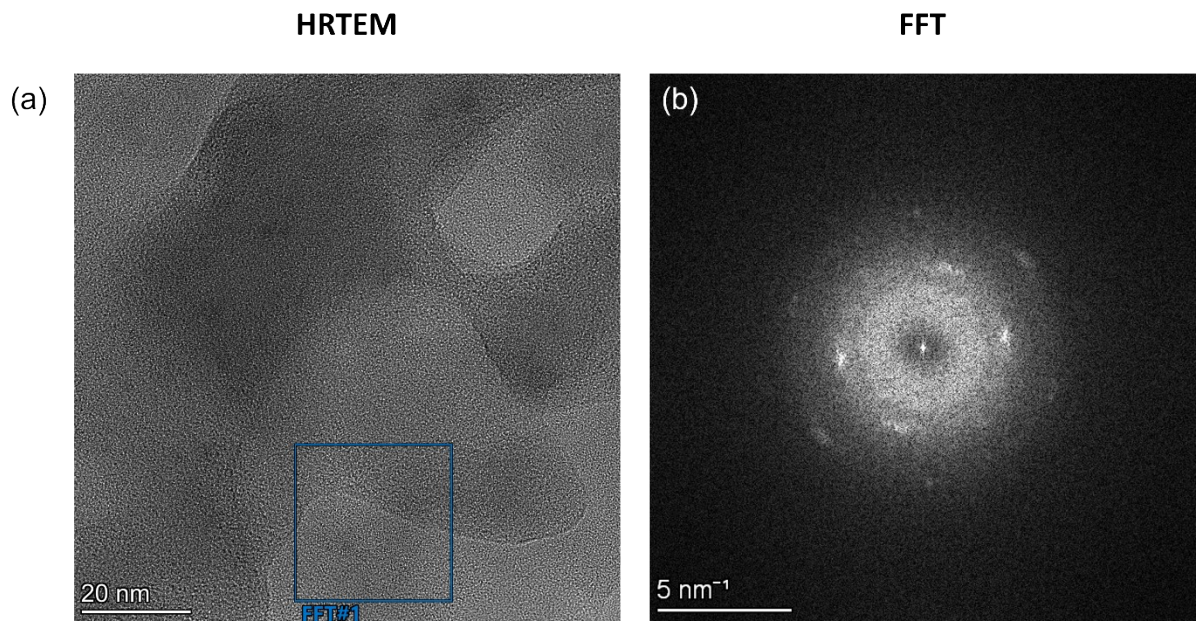

Figure S5: (a) High-Resolution TEM (HRTEM) image of the region with amorphous carbon presence and the corresponding FFT signature (b).

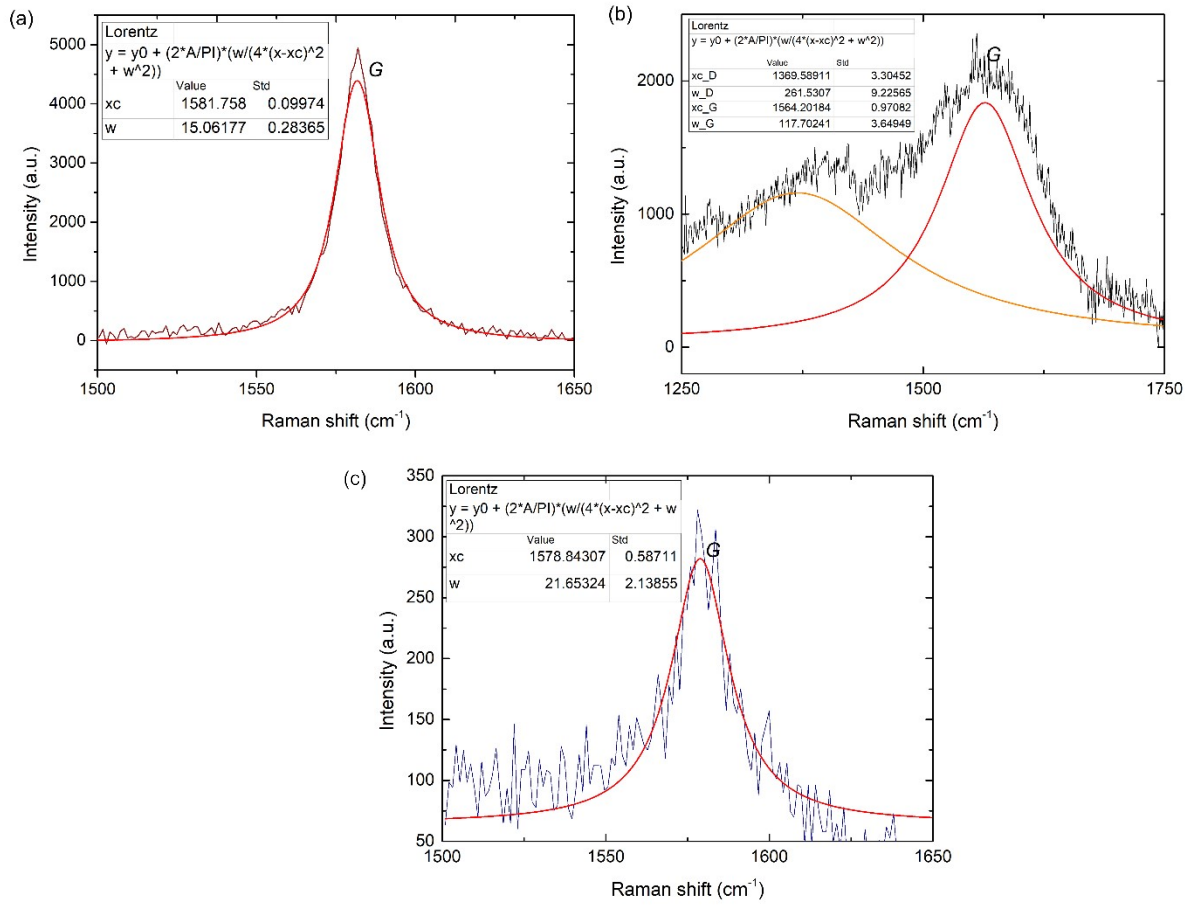

Figure S6: Lorentz fitting of the Raman *G* peak for (a) graphitic portion of the flakes (Fig. 6a in the main manuscript), (b) and (c) for the disordered portion of the flake flakes (Figs. 6b, c in the main manuscript). Insets show the Raman *G* peak fitting parameters, i.e., peak positions, xc and peak widths, w. All substrates are Si/SiO_2 with gold nanoparticles.

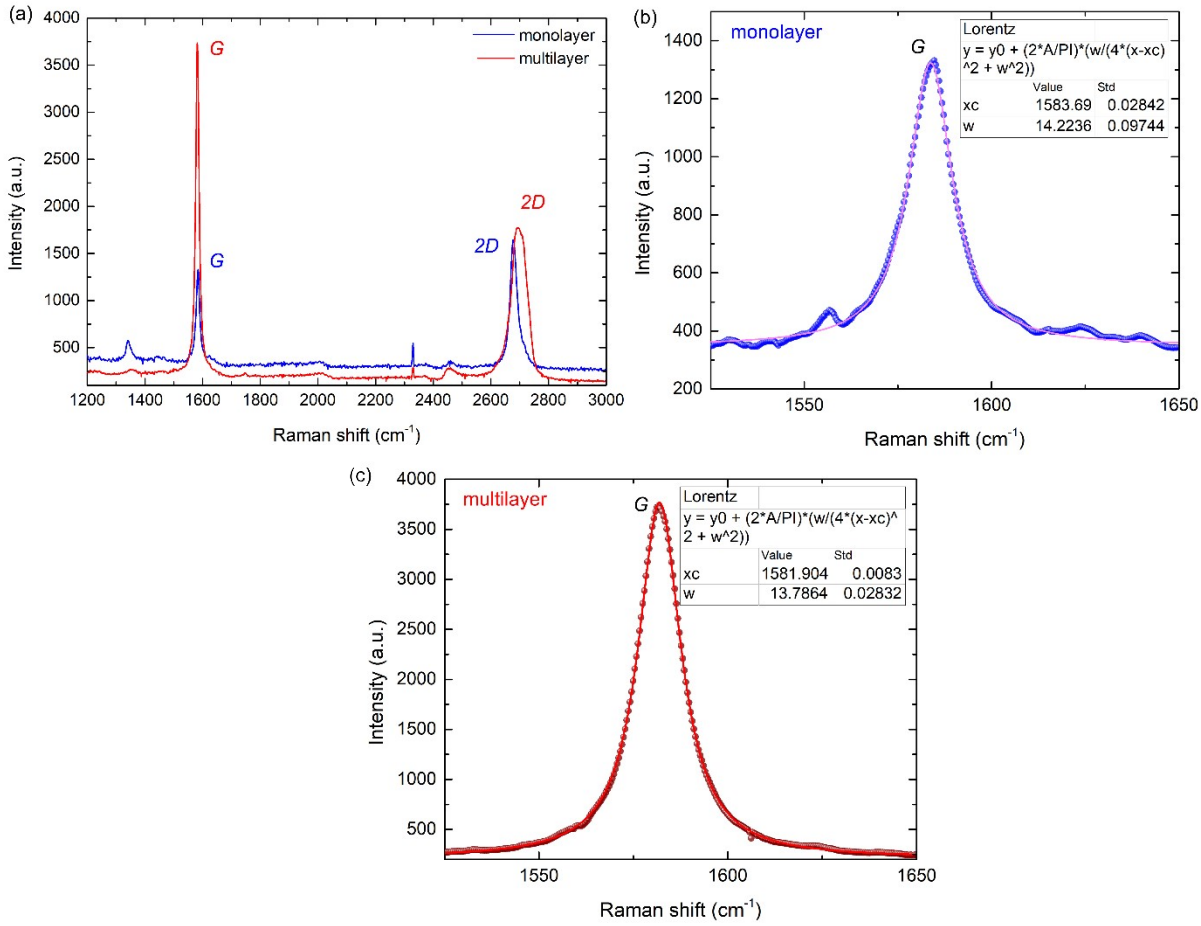

Figure S7: (a) Raman spectra of mechanically exfoliated monolayer and multilayer graphene on Si/SiO_2 substrates without any gold nanoparticles. The Raman *G* and *2D* peaks are shown for clarity. (b) Lorentz fitting of the Raman *G* peak for the monolayer graphene shown in (a). (c) Lorentz fitting of the Raman *G* peak for the multilayer graphene shown in (a). Insets show the Raman *G* peak fitting parameters, i.e., peak positions, xc and peak widths, w.

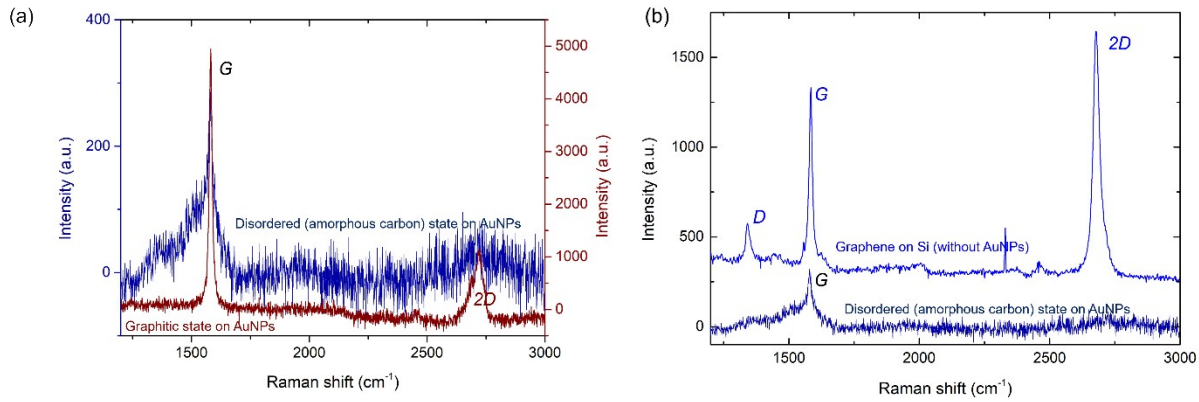

Figure S8: (a) Superimposed Raman spectra for the graphitic (Fig. 6a in the main manuscript) and disordered (Fig. 6c in the main manuscript) states for graphene on Si/SiO_2 substrates with gold nanoparticles. (b) Superimposed Raman spectra for the disordered (Fig. 6c in the main manuscript) states for graphene on Si/SiO_2 with gold nanoparticles and monolayer graphene on Si/SiO_2 substrates without any gold nanoparticles. The Raman *G, D,* and *2D* peaks are shown for clarity.

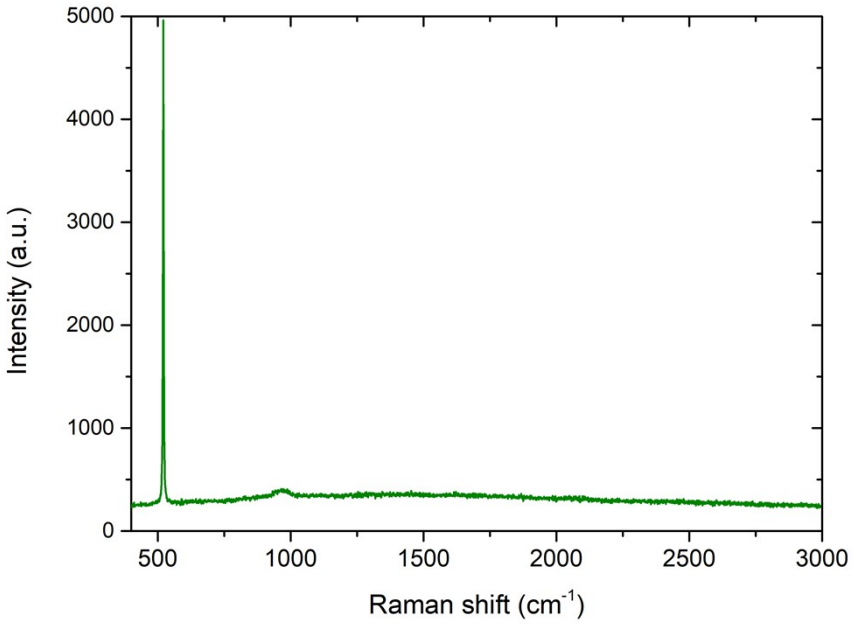

Figure S9: Raman spectrum of Si/SiO_2 substrates with gold nanoparticles without any graphene. The peak around 500 cm^{-1} Raman shift comes from the silicon substrate.

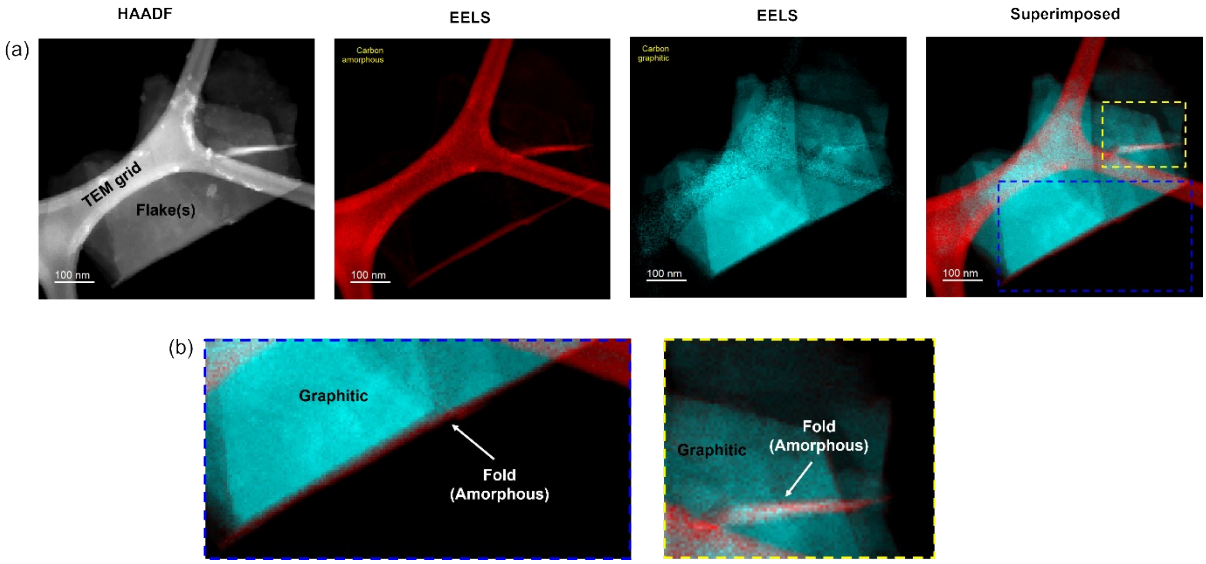

Figure S10: (a) HAADF image of graphene-only samples, i.e., without gold nanoparticles. Corresponding EELS elemental mapping signature of amorphous carbon and graphitic carbon. The final image is the superimposed elemental map of all the elements. The color assignment is arbitrary. (b) Enlarged views corresponding to the blue and yellow box regions in the superimposed image in (a), highlighting the amorphous carbon signature observed at the folds of the flake(s).